

Top and bottom emitting microcavity organic light emitting diode for enhancement of optical and electrical properties

N. Jain^{1*}, M. Dixit²

¹Department of Electrical and Electronics Engineering, Galgotias College of Engineering and Technology, Greater Noida, India

²Greater Noida Institute of Technology (Engineering Institute), Greater Noida, India

*Corresponding author e-mail: aceneha@gmail.com

Abstract. Microcavity effect in the structures has been used to enhance the optical and electrical characteristics of the device. A thin Ag layer between indium-tin-oxide (ITO) layers causes this effect with Ag acting as an internal reflector. Four device structures are designed and simulated. Two of them are top-emitting microcavity organic light emitting diodes (OLEDs) and the other two are bottom-emitting OLEDs. It has been observed at first comparison that indium-metal-indium structure with 20 nm thick Ag film has achieved maximum current density compared to the devices with other Ag film thicknesses. At this, an approximate increase in the current density values for the bottom-emitting OLED with aforementioned Ag layer thickness has amounted to 40%. Moreover, the top-emitting OLED with a zinc selenide capping layer at the cathode acting as a composite mirror to provide high reflectivity has had the highest electrical and optical output. The maximum achieved current density has been 1.2 A/cm². Furthermore, the electroluminescence intensity has enhanced by 33%.

Keywords: ZnSe, organic light emitting diode, indium-metal-indium structure, Ag, microcavity, J - V characteristics.

<https://doi.org/10.15407/spqeo29.01.118>

PACS 85.60.Jb

Manuscript received 05.06.25; revised version received 27.02.26; accepted for publication 18.03.26; published online 25.03.26.

1. Introduction

Light emitting diodes (LEDs) with layers of an organic electroluminescent material have various merits for displaying and lighting purposes such as high contrast ratio, fast response time, colour saturation, high efficiency, broad viewing angle *etc.* But the substitution of an inorganic material with an organic one to obtain the desired characteristics complicates the design of organic light emitting diodes (OLEDs). It is reported in [5] that the external quantum efficiency (EQE) of the OLED with a common structure design is only around 20%. The reasons for this may include mismatch of refractive indices, total internal reflection during light emission, and generation of surface plasma polaritons at the metal/dielectric interfaces [1, 5, 6]. The latter can be discussed in the framework of the classical ray optics as follows.

As reported in [4], the relative intensity of light that can be lost while passing a substrate, *i.e.* the external out-coupling efficiency $n_{cp,ext}$, is expressed as follows:

$$n_{cp,ext} \approx \frac{1}{2n_{org}^2}, \quad (1)$$

where n_{org} is the refractive index of the organic layer material.

The relative intensity of light trapped within the substrate $n_{cp,sub}$ and in the ITO/organic layers $n_{cp,org}$ are

$$n_{cp,sub} = \cos\theta_{org,c1} - \cos\theta_{org,c2}, \quad (2)$$

$$n_{cp,org} = \cos\theta_{org,c2}, \quad (3)$$

where $\theta_{org,c1}$ is the critical angle between the organic layer and air and $\theta_{org,c2}$ is the critical angle between the organic layer and the substrate, respectively. According to Eqs (2) and (3), a large amount of the generated light is emitted at the interfaces or only from the boundaries of the device. Most OLED manufacturers use microcavities to reduce losses of the light emitted from the device boundaries thus improving the device characteristics [4, 5].

Additional light extraction techniques can also be employed to enhance the EQE of the device. They include e.g. use of microcavities created by certain layers such as scattering layers (microlens arrays, photonic crystals) or capping layers such as ZnSe. The light extraction techniques may include use of optical diffusers, microlenses, microcavities, photonic crystals, nanoparticles, nanowires, nanostructures *etc.* Diffusers are mainly used in inorganic OLEDs [4–7, 21, 22]. Weak microcavity effect can also be employed. It is responsible

for both increased light outcoupling efficiency and broad viewing angle. A microcavity structure consists of a bottom mirror and can also include a top metal mirror. The bottom mirror is a distributed Bragg reflector, which defines the distribution of electric field modes and in this way increases the exciton spontaneous lifetime and, hence, the quantum efficiency. However, the microcavity effect also causes undesirable angular emission characteristics. Using diffusers instead of microlenses, colour and two-fold quantum efficiency can be improved. Moreover, use of diffuser films is much simpler. Another technique that can be employed for light enhancement is use of microlenses at the back surface of the substrate. The external out coupling increases by a factor of 1.5 by using ordered microlenses array and by 1.8 by using disordered microlenses array. The microlenses suppress wave guiding losses in the substrate. Another method to employ the microcavity effect is using a couple of low- and high-index layers between the glass and the ITO substrate. Such approach leads to an increase in the top reflectivity. Zinc selenide (ZnSe) can be added as a capping agent to form a low-absorption high-reflection composite mirror to maximize the optical output of the OLED device [1–7].

2. Device structure

Fig. 1 shows different structures used to enhance the desired OLED properties and simulated in the paper. Fig. 1a shows the structure where IMI (Indium-metal-indium) is used to induce the microcavity effect. In this structure, a thin Ag insert acts as a reflector to increase the device output. This is done by using an IMI electrode instead of merely ITO. Fig. 1b presents the structure, where further increase of the device characteristics was attempted by using an additional thin Ag layer at the cathode to enhance electron injection in the device. The Ag layer at the cathode acts as a semitransparent cathode. Both Figs. 1a and 1b refer to bottom-emitting microcavity OLEDs.

Figs. 1c and 1d present top-emitting microcavity OLEDs. For the structure shown in Fig. 1c, the Ag insert at the anode acts as a highly reflective layer. The maximum output from the device is achieved when a ZnSe layer is present after the Ag layer at the cathode side. The ZnSe layer is used to form a low-absorption highly reflective composite mirror, which increases the device efficiency.

The IMI properties are highly dependent on the intermediate layer, which is sandwiched between two ITO layers. Ref. [3] reports that silver is the best choice to use as an intermediate layer since it has high transmittance and conductivity even at very low layer thicknesses. It works as a weak reflective mirror which enhances the cavity effect [1, 3]. Fig. 1a shows a bottom-emitting OLED device with a microcavity layered structure. The thickness of the Ag intermediate layer in this structure is variable (x nm) to achieve the highest device output. The used values of x are 5, 20, 30 and 35 nm. The thickness of 5 nm is called the first order cavity length. This value is too small to ensure stable device operation.

1, 4, 5, 8, 9, 11-hexaazatriphenylene-hexacarbonitrile (HAT-CN) in the device structure acts as a hole injection layer (HIL). The HIL effectively modifies the electronic characteristics of the device. Namely, it results in a drastic increase in the current density of the device. 1, 4, 5, 8, 9, 11-hexaazatriphenylene-hexacarbonitrile (HAT-CN) acts as an intermediate layer between the substrate and the hole transport layer (HTL). 2, 7-bis [N, N-bis (4-methoxy-phenyl) amino]-9, 9-spirobifluorene (meo-spiro TPD) is used as the HTL. Tris(8-hydroxyquinolate) aluminium (Alq₃) acts as the light emitting layer (EML) as well as the electron transport layer (ETL). A host-guest system is employed in the device. It is created by doping 4,4'-N,N dicarbazolylbiphenyl (CBP) with 5% fac-Tris(2-phenylpyridine)iridium (Ir(ppy)₃). CBP as a host and Ir(ppy)₃ as a guest increase phosphorescence of the device. Alq₃ is responsible for green light emission from the device. An ultrathin layer of lithium fluoride/aluminium (LiF/Al) is used as a cathode, which acts as an electron injection layer (EIL). LiF is applied to solve problems with low corrosion resistance materials. An Al/Ag layer at the cathode in the device structures C and D is also responsible for enhancing electron injection [1, 10].

Fig. 1b shows a device using the microcavity effect with a semitransparent Ag layer at the cathode. Here, the IMI acts as a waveguide (internal reflector) to enhance emission. Fig. 1c shows a device with a thin Ag layer serving as a semitransparent top cathode. In Fig. 1d, the Ag cathode is further capped with ZnSe, which forms a high-reflection low-absorption composition mirror. Use of ZnSe enables improving the required device characteristics, which will be described below.

3. Mathematical model

In our simulations, we used the Poole–Frenkel mobility model, Shockley–Read–Hall recombination model and Richardson thermionic emission model. According to the former model, the carrier mobility (μ) is dependent on the electric field (F) as follows:

$$\mu = \mu_0 \exp\left(\sqrt{\frac{F}{E_0}}\right), \quad (4)$$

where μ_0 is the zero-field mobility and E_0 is a constant.

The Richardson thermionic emission law is used for current injection. The current density can be represented as follows:

$$J = AT^2 \exp\left\{\frac{-\phi_b - \beta\sqrt{F}}{kT}\right\}, \quad (5.1)$$

which can be expressed in terms of the surface recombination velocity as

$$J = A^*T^2 \exp(-\phi/kT) - enS, \quad (5.2)$$

Here, A^* is the Richardson constant, T is the temperature, ϕ is the barrier height over which the carriers have to be injected, k is the Boltzmann constant, e the electron charge, n is the charge density at the contact, and S is the surface recombination velocity, respectively. The Richardson constant for electrons (A_n^*) and holes (A_p^*) can be defined as

(a)	(b)	(c)	(d)
ITO (50 nm)	ITO (50 nm)	ITO (50 nm)	ITO (50 nm)
Ag(5nm)	Ag(5nm)	Ag(5nm)	Ag(5nm)
ITO (50nm)	ITO (50nm)	HAT-CN (5nm)	HAT-CN (5nm)
HAT-CN (5nm)	HAT-CN (5nm)	Meo-Spiro-TPD (9nm)	Meo-Spiro-TPD (9nm)
Meo-Spiro-TPD (9nm)	Meo-Spiro-TPD (9nm)	CBP doped with Ir(ppy) ₃ (25nm)	CBP doped with Ir(ppy) ₃ (25nm)
CBP doped with Ir(ppy) ₃ (25nm)	CBP doped with Ir(ppy) ₃ (25nm)	Alq ₃ (22nm)	Alq ₃ (22nm)
Alq ₃ (22nm)	Alq ₃ (22nm)	LIF (1nm)	LIF (1nm)
LIF (1nm)	LIF (1nm)	AI (10nm)	AI (10nm)
AI (100nm)	AI (10nm)	Ag(20nm)	Ag(20nm)
	Ag(20nm)		ZnSe (45nm)

Fig. 1. Device structures of (a) bottom-emitting microcavity OLED, (b) bottom-emitting microcavity OLED with an Ag layer at the cathode, (c) top-emitting microcavity OLED, (d) top-emitting microcavity OLED with a ZnSe layer as a high-reflection composite mirror.

$$A_n^* = \frac{4\pi q k^2 m_n^*}{h^3}, \quad (6)$$

$$A_p^* = \frac{4\pi q k^2 m_p^*}{h^3}. \quad (7)$$

Here, m_n^* and m_p^* are the electron and hole effective masses, respectively. Generally, the value of this constant is $1.18 \cdot 10^2 \text{ A/cm}^2 \text{ K}^2$ for both holes and electrons.

The surface recombination velocity S at zero electric field, can be defined as follows:

$$S(0) = 16\pi\epsilon\epsilon_0 (kT)^2 \mu / e^3, \quad (8)$$

where μ is the charge mobility and $\epsilon\epsilon_0$ is the dielectric constant, respectively.

At applied electric field, the recombination velocity becomes

$$S(E) = S(0) \left(\frac{1}{\Psi^2} - f \right) / 4. \quad (9)$$

Here, f is the reduced field and Ψ is the injection current at the metal/organic interface, respectively.

According to the Shockley–Read–Hall recombination model under steady-state conditions

$$\frac{1}{\tau_p(x)} = \int_{E_{\text{HOMO}}}^{E_{\text{LUMO}}} dE \frac{J \sigma_p N_t(E) / q N_{\text{LUMO}}}{\exp[(E_n(x) - E_{\text{LUMO}}) / kT] + \exp[(E - E_{\text{LUMO}}) / kT]}, \quad (10)$$

where σ_p is the hole capture cross-section, which is assumed to be independent of temperature and energy. Given $n(x)$ the density of electrons in Lowest Unoccupied Molecular Orbital (LUMO)

$$E_n(x) = E_{\text{LUMO}} - kT \ln \left(\frac{n(x)}{N_{\text{LUMO}}} \right), \quad (11)$$

The dependence $n(x)$ can be calculated by simultaneously solving the Poisson and continuity equations. In this work, this is done by using a regional approximation model [10–13].

All the simulations in this work were carried out using Silvaco TCAD tool.

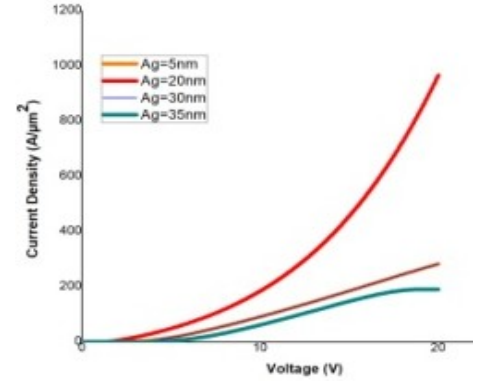


Fig. 2. J – V characteristics of OLEDs with different thicknesses of Ag layer.

4. Results and discussions

The four-layer nano-OLED device structures shown in Fig. 1 have been simulated to find out the ways to enhance the OLED electro-optical characteristics. At this, if the light is emitted from the substrate side, the device is called bottom-emitting OLED. If light emission takes place from the cathode side, it is a top-emitting device.

Fig. 2 shows J – V characteristics of the devices with different Ag layer thicknesses. It can be seen from this figure that the microcavity device with the Ag layer thickness of 20 nm has the maximum current density. This thickness is called the second-order cavity length. At this, however, the microcavity device with this type of the metal insertion has some drawbacks. For example, luminance in such cases increases in a particular direction with respect to luminance distribution where this distribution is angular in nature. Another drawback is the increase in the spectral distortion in case of IMI microcavity OLEDs [1].

Fig. 3 shows J – V characteristics of the device structures shown in Fig. 1. The device A is the structure with an Ag insert between the ITO substrates demonstrating the microcavity effect. The device B is the structure with an additional Ag layer acting as semitransparent cathode. It can be seen from Fig. 3 that

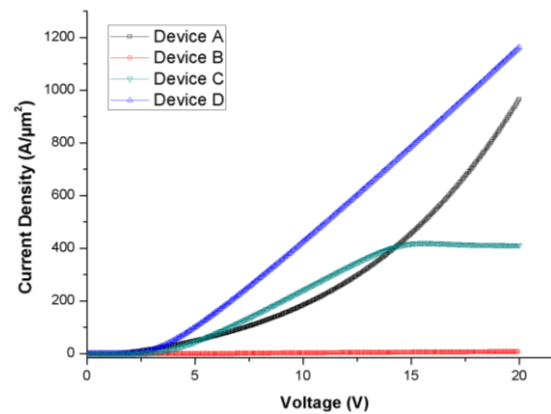


Fig. 3. J – V characteristics of different device structures.

Ag layer inserted at the cathode side has no effect for a bottom-emitting microcavity OLED, and the current density of the device B significantly decreases. In the device C, the Ag layer at the anode acts as a highly reflective layer and the Ag layer at the cathode acts as a semitransparent top cathode. Therefore, it is a top-emitting microcavity OLED. In this device, an Al/Ag layer at the cathode improves the electron injection in the device and, hence, the device performance. The device output can be further enhanced by changing the Al/Ag ratio. This issue is out of scope of this work and will be considered elsewhere. The result presented in Fig. 3 signifies high reflectivity of Ag layers at long wavelengths. The device D is the structure with a ZnSe layer added at the cathode side and serving as a low-absorption highly reflective composite mirror used to increase the device optical output. It can be seen from Fig. 3 that the device D has the highest electrical output. The ZnSe layer in the device D acts as a capping layer (CL). Such layers are used with organic/inorganic materials to modify reflection and absorption of the device and to improve its transmittance. ZnSe has high refractive index ($n = 2.5$) and, hence, increases the device optical output based on the total internal reflection concept between the CL and air ($n = 1$). The results presented in Fig. 3 clearly show that ZnSe as a CL leads to enhanced interaction of holes and electrons.

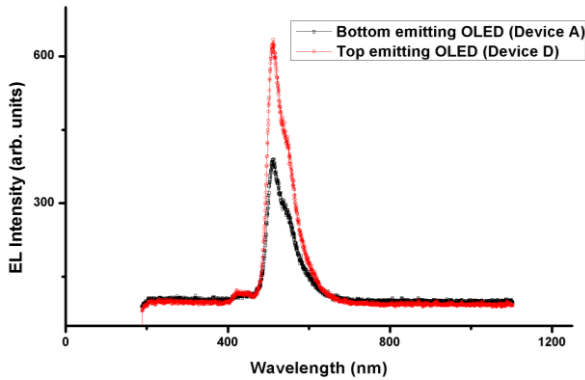


Fig. 4. Electroluminescence intensity versus wavelength for top- and bottom-emitting OLEDs.

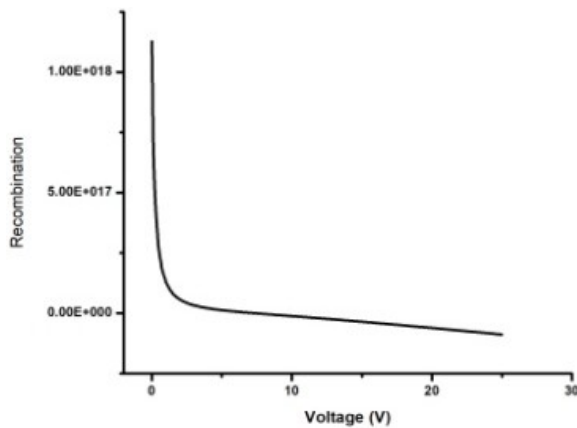


Fig. 5. Recombination vs applied voltage for an OLED structure.

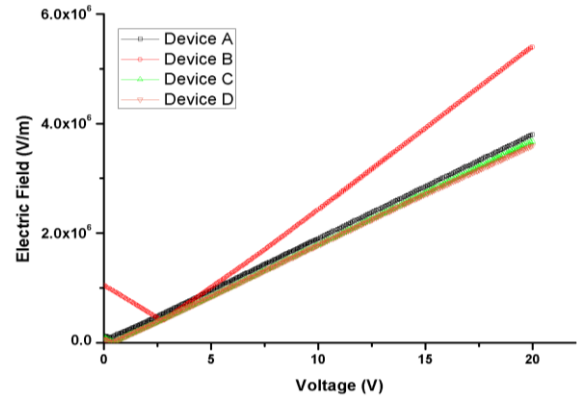


Fig. 6. Electric field vs applied voltage for different devices.

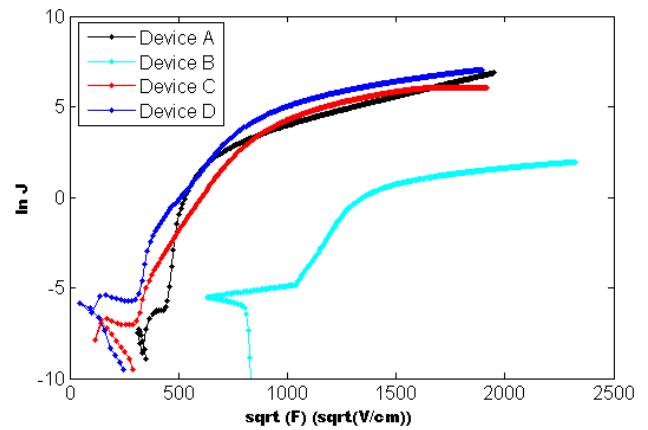


Fig. 7. \sqrt{F} versus $\ln(J)$ for different devices.

The device performance can be further controlled by optimizing the CL thickness. It was reported in [17] that adding a thin scattering ZnSe layer as a CL increases the stability of emission with high efficiency [14–18].

Fig. 4 shows comparison of electroluminescence intensity for top- and bottom-emitting OLED devices. It can be seen from this figure that the top-emitting OLED with the ZnSe layer as the highly reflective mirror at the cathode side exhibits a higher electroluminescence intensity as compared to the conventional bottom-emitting diodes A and B.

Fig. 5 shows the recombination velocity versus applied voltage. The behaviour of this characteristic is attributed to excited cavernous and shallow trap levels and, hence, the change in the recombination zone. The recombination zone changes as the voltage increases, which adds an effect on the recombination efficiency. That is, an increase in the voltage induces a decrease in the recombination efficiency. This is attributed to a reduced interfacial energy barrier, which enhances the hole current density at the anode/organic layer interface [23]. Furthermore, the electric field steadily increases from the ITO/EML interface with the applied voltage along the EML as shown in Fig. 6, which also influences the dependence of recombination on the voltage at the EML [20]. A linear increase in the electric field with applied voltage can be seen in Fig. 6, which implies that

the properties of the organic materials in the device are dependent on the electric field. Furthermore, Fig. 7 shows \sqrt{F} as a function of logarithm of current density. It can be concluded from Fig. 5 that the device B has the highest electric field with respect to the voltage as compared to the devices A, C and D.

It can be seen from Fig. 7 that the dependence $\sqrt{F}(\ln J)$ is almost linear. This linearity confirms thermionic injection of charge carriers in OLED. It should be noted as well that the data in Figs. 5 and 7 have been obtained for the same values of applied electric field used. As can be further seen from Fig. 7, the values of \sqrt{F} are the lowest for the device B, which is caused by the smallest injection of charge carriers. This conclusion is confirmed by the data presented in Fig. 3, which show the lowest current densities for the device B.

5. Conclusions

In summary, we show that by using ZnSe as a reflective fused mirror, the opto-electrical characteristics of top-emitting microcavity OLEDs can be improved. An increase in the electrical characteristics of the device with a 20 nm Ag layer by approximately 60% as compared to the devices with other Ag layer thicknesses is demonstrated (see Fig. 2). The device D has been found to have the highest current density of 1.2 A/cm² as compared to other devices because of high reflection provided by a ZnSe layer at the cathode acting as a composite mirror. Therefore, the electroluminescence intensity of the device D increases by nearly 35% as compared to the device C the only difference of which was absence of ZnSe layer. Thermionic emission of charge carriers is evidenced by electric field dependence of the current density. The features of ZnSe make it an attractive material to use as a cathode for enhancements of optical and electrical properties of device structures for future applications.

References

- Joo C.W., Lee K., Lee J. *et al.* Optical and structural approaches for improved luminance distribution and enhanced efficiency of organic light emitting diodes. *J. Lumin.* 2017. **187**. P. 433–440. <https://doi.org/10.1016/j.jlumin.2017.03.057>.
- Cho S.-H., Song Y.-W., Lee J. *et al.* Weak-microcavity organic light-emitting diodes with improved light out-coupling. *Opt. Express*. 2008. **16**, No 17. P. 12632–12639. <https://doi.org/10.1364/OE.16.012632>.
- Chen S.-W., Koo C.-H., Huang H.-E., Chen C.-H. Ag–Ti alloy used in ITO–Metal–ITO transparency conductive thin film with good durability against moisture. *Mater. Trans.* 2005. **46**, No 11. P. 2536–2540. <https://doi.org/10.2320/matertrans.46.2536>.
- Mehta D.S., Saxena K. Light out-coupling strategies in organic light emitting devices. *Proc. ASID'06, 8-12 Oct, New Delhi*.
- Pyo B., Joo C.W., Kim H.S. *et al.* A nanoporous polymer film as a diffuser as well as a light extraction component for top emitting organic light emitting diode with strong microcavity structure. *Nanoscale*. 2016. **8**. P. 8575–8582. <https://doi.org/10.1039/C6NR00868B>.
- Liu C.-C., Liu S.-H., Tien K.-C. *et al.* Microcavity top-emitting organic light-emitting devices integrated with diffusers for simultaneous enhancement of efficiencies and viewing characteristics. *Appl. Phys. Lett.* 2009. **94**. P. 103302. <https://doi.org/10.1063/1.3097354>.
- Saxena K., Jain V.K., Mehta D.S. A review on the light extraction techniques in organic electroluminescent devices. *Opt. Mater.* 2009. **32**. P. 221–233. <https://doi.org/10.1016/j.optmat.2009.07.014>.
- Poitras D., Kuo C.-C., Py C. Design of high-contrast OLEDs with microcavity effect. *Opt. Express*. 2008. **16**, No 11. P. 8003–8015. <https://doi.org/10.1364/OE.16.008003>.
- Rajan G., Yadav V., Manzhi P. *et al.* Study of injection and transport properties of metal/organic interface using HAT-CN molecules as hole injection layer. *Vacuum*. 2017. **146**. P. 530–536. <https://doi.org/10.1016/j.vacuum.2017.07.007>.
- Jain N., Sinha O.P., Pandey S. Optimization of organic light emitting diode for HAT-CN based nano-structured device by study of injection characteristics at anode/organic interface. *Front. Optoelectron.* 2019. **12**. P. 268–275. <https://doi.org/10.1007/s12200-019-0848-y>.
- Hsiao C.-H., Chen Y.-H., Lin T.-C. *et al.* Recombination zone in mixed-host organic light-emitting devices. *Appl. Phys. Lett.* 2006. **89**. P. 163511. <https://doi.org/10.1063/1.2361266>.
- Malliaras G.G., Scott J.C. Numerical simulations of the electrical characteristics and the efficiencies of single-layer organic light emitting diodes. *J. Appl. Phys.* 1999. **85**, No 10. P. 7426–7432. <https://doi.org/10.1063/1.369373>.
- Burrows P.E., Shen Z., Bulovic V. *et al.* Relationship between electroluminescence and current transport in organic heterojunction light emitting devices. *J. Appl. Phys.* 1996. **79**. P. 7991–8006. <https://doi.org/10.1063/1.362350>.
- Lee J.-W., Lee J., Chu H.Y. & Lee J.-I. Controlling the optical efficiency of the transparent organic light-emitting diode using capping layers. *Journal of Information Display*. 2013. **14**, No 2. P. 57–60. <https://doi.org/10.1080/15980316.2013.783512>.
- Riel H., Karg S., Beierlein T. *et al.* Phosphorescent top-emitting organic light-emitting devices with improved light outcoupling. *Appl. Phys. Lett.* 2003. **82**, No 3. P. 466–468. <https://doi.org/10.1063/1.1537052>.
- Rieß W., Beierlein T.A., Riel H. Optimizing OLED structures for a-Si display applications via combinatorial methods and enhanced outcoupling. *phys. status solidi (a)*. 2004. **201**, No 6. P. 1360–1371. <https://doi.org/10.1002/pssa.200404347>.
- Hofmann S., Thomschke M., Lüssem B., Leo K. Top-emitting organic light-emitting diodes. *Opt. Express*. 2011. **19**, No S6. P. A1250–A1264. <https://doi.org/10.1364/OE.19.0A1250>.

18. Kwon S.-K., Lee E.-H., Kim K.-S. *et al.* Efficient micro-cavity top emission OLED with optimized Mg:Ag ratio cathode. *Opt. Express*. 2017. **25**, No 24. P. 29906–29915. <https://doi.org/10.1364/OE.25.029906>.
19. Black L.E. *New Perspective on Surface Passivation: Understanding the Si-Al₂O₃ Interface*. Springer, 2016. <https://doi.org/10.1007/978-3-319-32521-7>.
20. Chowdhury R., Haq M.R., Chowdhury M.S.U. *et al.* Effect of higher carrier injection rate on charge transport and recombination in mixed-host organic light emitting diode. *2016 Int. Conf. on Innovations in Science, Engineering and Technology (ICISSET)*. <https://doi.org/10.1109/ICISSET.2016.7856493>.
21. Park C.H., Kang S.W., Jung S.G. *et al.* Enhanced light extraction efficiency and viewing angle characteristics of microcavity OLEDs by using a diffusion layer. *Sci. Rep.* 2021. **11**. P. 3430. <https://doi.org/10.1038/s41598-021-82753-9>.
22. Kumar M., Dutta A., Qureshi H.A. *et al.* Single-emitter white OLEDs via microcavity spectral engineering. *Adv. Opt. Mater.* 2025. **13**. P. e01358. <https://doi.org/10.1002/adom.202501358>.
23. Xu X., Peng J., Li H. *et al.* Effect of temperature and applied voltage on the recombination efficiency in double layer organic light emitting diodes. *PubMed*. 2004. **24**, No 1. P. 12-4.

Authors' contributions

Neha Jain: formal analysis, investigation, data curation (partially), visualization, validation, writing – original draft, writing – review & editing.

Monika Dixit: conceptualization, methodology, validation, formal analysis, investigation, resources, data curation, writing – original draft, writing – review & editing.

Authors and CV



Neha Jain, Associate Professor at the Department of Electrical and Electronics Engineering, Galgotias College of Engineering and Technology, Greater Noida. She received her PhD degree from the Amity University, Noida in 2021.

The main area of her research is simulation and fabrication of nano-structured devices for optoelectronic applications and study of their electrical and optical properties. Her interests also include organic materials, nano-structures and devices, organic electronics *etc.* She authored over 13 publications in reputed scientific journals and conference proceedings. She has organized many industry-related faculty development programs and workshops. E-mail: neha.jain@galgotiacollege.edu, <https://orcid.org/0000-0002-0976-3181>



Monika Dixit, Associate Professor at the Greater Noida Institute of Technology, Greater Noida (Uttar Pradesh). She defended her PhD thesis in VLSI Design (Semiconductor Physics) in 2022 at the Amity University, Noida. She authored over 30 publications, 8 patents, and 1 textbook. The area of her scientific interests includes frequency synthesizers, PLL, semiconductor materials *etc.* in VLSI Domain. She has successfully organized many industry-related workshops, faculty development programs and conferences. She has extensive knowledge in the electronics-related real time projects. She has filed many patents and research papers during her service.

E-mail: monika19electrical@gmail.com, <https://orcid.org/0000-0002-1533-0323>

Органічний світлодіод з верхнім та нижнім випромінюючими мікрорезонаторами для покращення оптичних та електричних властивостей

N. Jain, M. Dixit

Анотація. Ефект від мікрорезонаторів у структурах було використано для покращення оптичних та електричних характеристик пристрою. Цей ефект зумовлено наявністю тонкого шару срібла між шарами оксиду олова-індію (ITO), який використовується як внутрішній відбивач. Розроблено та змодельовано чотири приладні структури, дві з яких є органічними світлодіодами (OLED) з мікрорезонатором з верхнім випромінюванням, а дві інші – OLED з нижнім випромінюванням. Було показано, що у структурі індій-метал-індій з шаром срібла товщиною 20 нм досягається максимальна густина струму порівняно з пристроями з іншими значеннями товщини шару срібла. При цьому збільшення густини струму в OLED з нижнім випромінюванням з шаром срібла вищезазначеної товщини становило приблизно 40%. Крім цього OLED з верхнім випромінюванням з покривним шаром з селеніду цинку на катоді, що використовувався як композитне дзеркало для забезпечення високої відбивної здатності, мав найвищу електричну та оптичну ефективність. Максимальне досягнуте значення густини струму становило 1.2 А/см², а інтенсивність електролюмінесценції зросла на 33%.

Ключові слова: ZnSe, органічний світлодіод, структура індій-метал-індій, мікрорезонатор, Ag, *J-V* характеристики.